Civil Engineering
Engenharia Civil

Numerical analysis of cold-formed double angles back-to-back under compression

http://dx.doi.org/10.1590/0370-44672016700183

Davi Fagundes Leal
Professor
Instituto Federal de Educação, Ciência e Tecnologia Fluminense (IFF)
Campos dos Goytacazes - Rio de Janeiro - Brasil
Universidade de São Paulo – USP
Escola de Engenharia de São Carlos (EESC / USP)
Departamento de Engenharia de Estruturas (SET)
São Carlos - São Paulo – Brasil
daviufv@yahoo.com.br

Jorge Munaiar Neto
Professor Associado
Universidade de São Paulo – USP
Escola de Engenharia de São Carlos (EESC / USP)
Departamento de Engenharia de Estruturas (SET)
São Carlos - São Paulo - Brasil
jmunaiar@sc.usp.br

Maximiliano Malite
Professor Titular
Universidade de São Paulo – USP
Escola de Engenharia de São Carlos (EESC / USP)
Departamento de Engenharia de Estruturas (SET)
São Carlos - São Paulo - Brasil
mamalite@sc.usp.br

Abstract

Here-in, a numerical analysis based on the Finite Element Method (FEM) is proposed in order to investigate cold-formed steel back-to-back double angle structural behavior under compression. Considering non-linear analysis, an investigation was performed to analyze the influence of some aspects, such as the loading condition (concentric and eccentric axial compression), the boundary conditions, the global slenderness, the global and local geometric imperfections, the angle thickness and the number of packing plates. The numerical results signalize that the compression strength obtained in accordance with the standards ABNT NBR 14762:2010 and ANSI/AISI S100 (2012) may be quite conservative, mainly in the lower global slenderness cases. Additionally, the connection spacing (bolted connection with stitch plates in-between the angles) and the presence of a connection at mid-length change the buckling mode, as well as cause a significantly increase in the axial compression strength of the member. The numerical analysis also indicates that the design proposed by ABNT NBR 8800:2008 for the case involving angles under compression connected by one flap can also be applied to cold formed steel angles.

Keywords: steel structures, cold-formed steel angles, structural stability, numerical analysis, non-linear analysis.

1. Introduction

Among all cold-formed steel profiles applied in common structural systems, it is worth highlighting those that are back-to-back double angle bounded with the use of packing plates. Although they are highly used, their structural behavior needs to be better analyzed, mainly concerning the instability modes associated with them. Therefore, the goal of this work is to improve the understanding about the structural behavior of the referred profiles and to contribute in future reviews to the Technical Standards of ABNT NBR 14762:2010.

2. Methodology

Numerical models were developed using the resources of the computational codes ANSYS and analyzed through the Finite Element Method, considering the geometric and material nonlinearities. Initially, members submitted to axial compression were analyzed, from which the numerical model was calibrated by comparison to the experimental results presented in Chodraui (2006) and Chodraui *et al.* (2006). In a second step, the structural behavior of the members was investigated under eccentric compression, which more commonly characterizes the practice applied in civil building construction. The range of analysis considered members with slenderness range usually identified in the engineering practice. Additional information about the methodology here-in presented can be obtained in Leal (2011).

2.1 Geometry of the models

To perform the evaluation of local buckling slenderness (width-to-thickness ratio of the plates) influence on the members behavior, plates considering two different thickness were analyzed, i.e., two different cross sections with dimensions 60x60x1.5 mm and 60x60x3.0 mm (Figure 1). The distance between the angles, defined by thickness of packing

plates, was fixed in 5.0 mm. The rounded corners, resultant of the manufacturing process, were modeled with a mid-line radius of the walls equal in proportion to 1.5 of plate thickness. Maintaining the dimensions of both cross sections presented, the global buckling slenderness was considered by varying the member length. Thus, the profiles were analyzed with a slenderness ratio (*KL/r*) from 20 to 160.

The number of packing plates used was adopted from zero (0), i.e, back-to-back double angle connected only by the support devices (end connections), up to four (4). The support devices (end connections) were modeled with solid elements on tops clamped and connected to the bonding plate at each extremity. The end section eccentric loading was applied with a single 19mm bolt connection in one flap.

2.2 Mesh and finite elements

The mesh discretization was developed using, basically, three finite elements available in the ANSYS library: **SHELL 181** for angles plate, **SOLID 45** for the solids of the ends and packing plates, as well as **SOLID 95** for plate connections.

From the test results, mapped element mesh of approximately 1 x 1 cm^2 was inserted, except in the connection mesh, where triangular shape elements were used to describe the hole borders with more accuracy. Additionally, in order to eliminate the possibilities of plate interpenetration, pairs of contact elements equivalent to the base elements were also used, i.e., **CONTA 173** and **TARGE 170** for **SHELL 181** and **SOLID 45** elements mesh, as well as **CONTA 174** and **TARGE 170** for meshes with elements **SOLID 95**, as represented in the Figure 2.

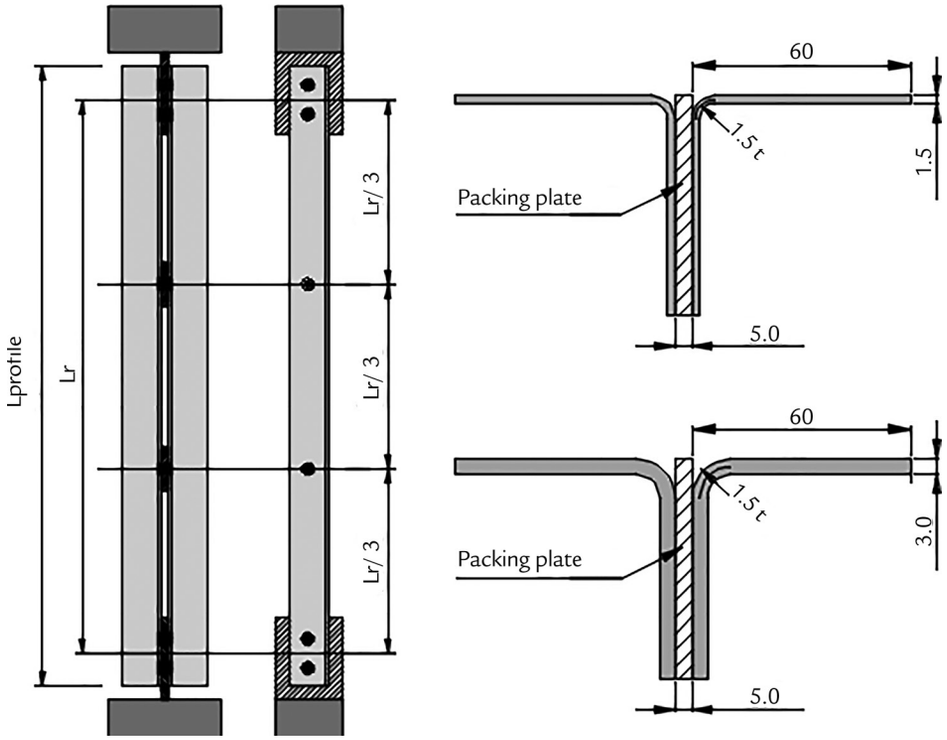

Figure 1
Numerical Models Geometry: profiles with two packing plates and cross-sections.

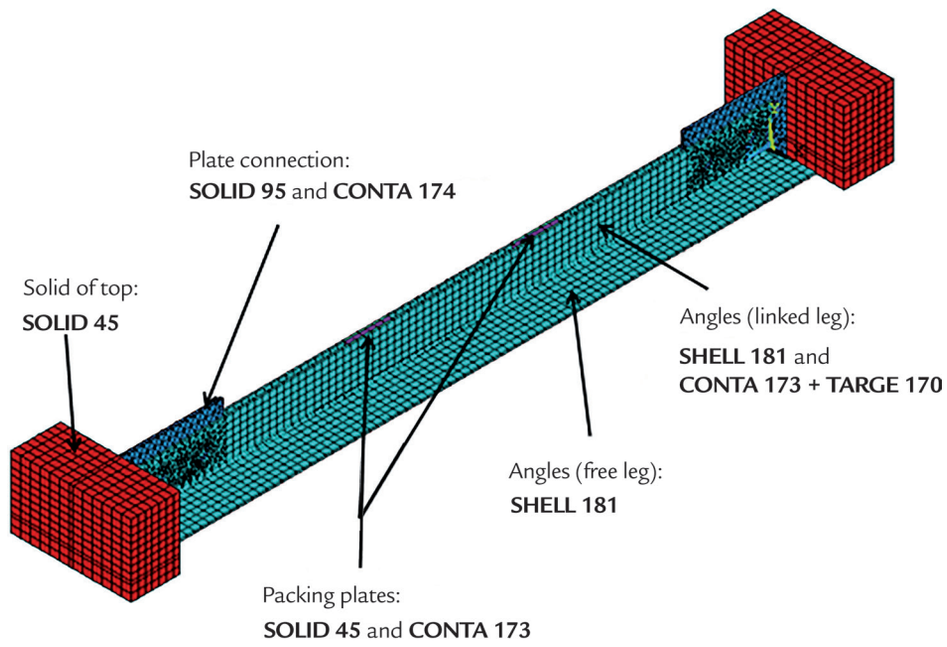

Figure 2
Mesh and finite elements used in the numeric models.

2.3 Geometric imperfections

According to Leal (2011), a considerable amount of sensibility analysis was conducted to identify geometric imperfections that describe with more accuracy the behavior of members, when it is correlated with the experimental results presented in Chodraui (2006). Figure 3 shows the shape of the global and local geometric imperfections added in the numerical models, resulting in an association of local/torsional and global bending imperfections. The magnitude of the initial geometric imperfections was evaluated with L/1500 and L/1000 for the global bending imperfection and 0.64t and 0.94t for the local imperfections (where L is the profile length and t is the thickness plate), as proposed in Schafer and Peköz (1998).

2.4 Materials used

For the angles, the end connections and the packing plates, a steel constitutive stress-strain curve was adopted based on both yield strength fy = 350 MPa and tensile strength fu = 498 MPa (Figure 4). The nominal values were adjusted in accordance with Hancock and Yang (2004), in which the variation in the resistance area for large deformation cases is considered to obtain the curve with corrected values.

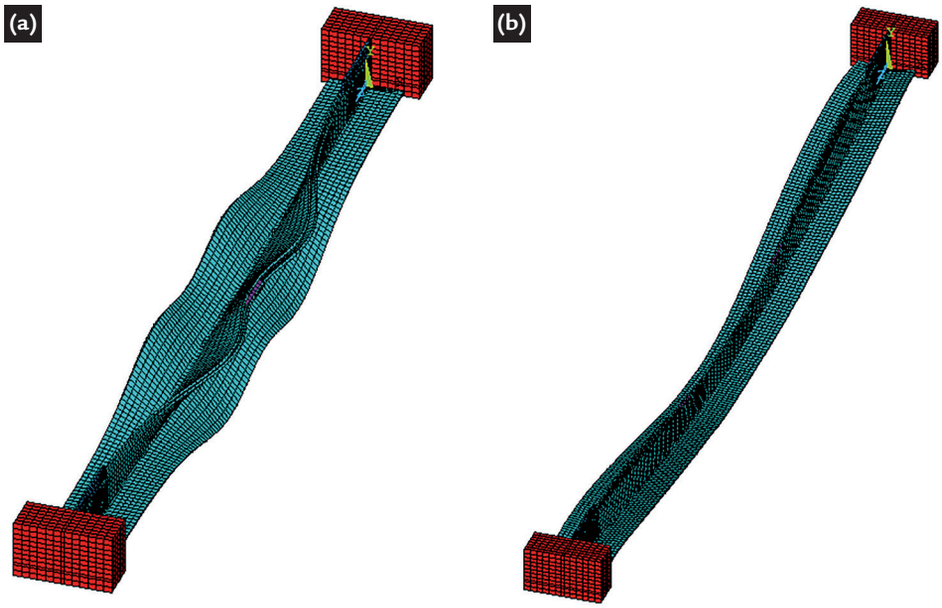

Figure 3
Expanded scale of the initial geometric imperfections (a) local/torsional e (b) global bending.

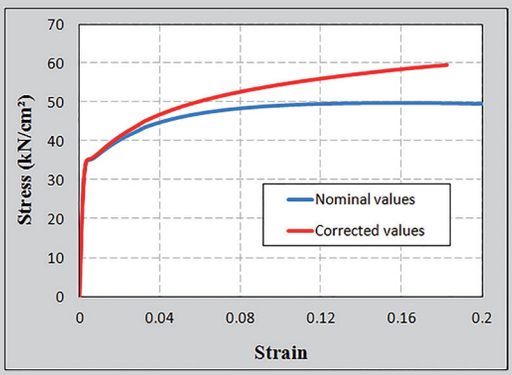

Figure 4
Stress-strain curve used in the models.

3. Numerical model validation

In order to calibrate the numerical model, analyses were performed and their results compared to the results obtained from the experimental program presented in Chodraui *et al.* (2006), for axially compressed 60x60x2.38mm double angles.

Figures 6 and 7 present the numerical model results compared to the respective experimental tests, based on two analyzed profiles, where similar collapse modes between the numerical and experimental results are observed in both cases. As theoretical predictions relative to elastic buckling analysis for monosymmetric cross-section profiles, notice a change in the predominant instability mode when increasing the members' slenderness ratio, prevailing the flexural-torsional buckling for profiles with lower slenderness (Figure 5) and the flexural buckling for more slender members (Figure 6). For these cases, the axial compression strength ratio between experimental and numerical results (Ntest / NFEM) was, on average, equal to 0.92 and 0.97, respectively.

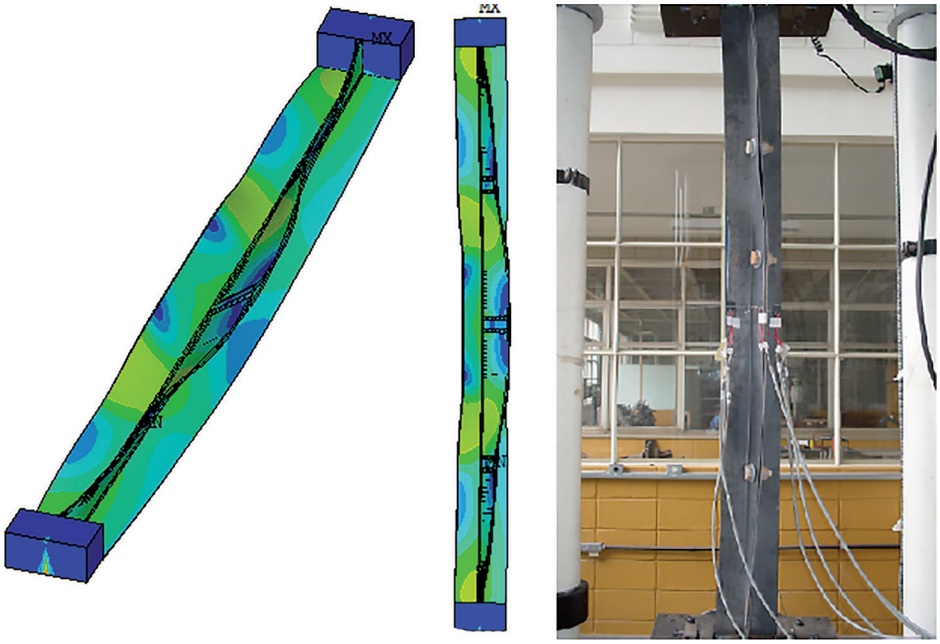

Figure 5
Deformed shape to L_r = 1490mm: numerical model and experimental test from Chodraui *et al.* (2006).

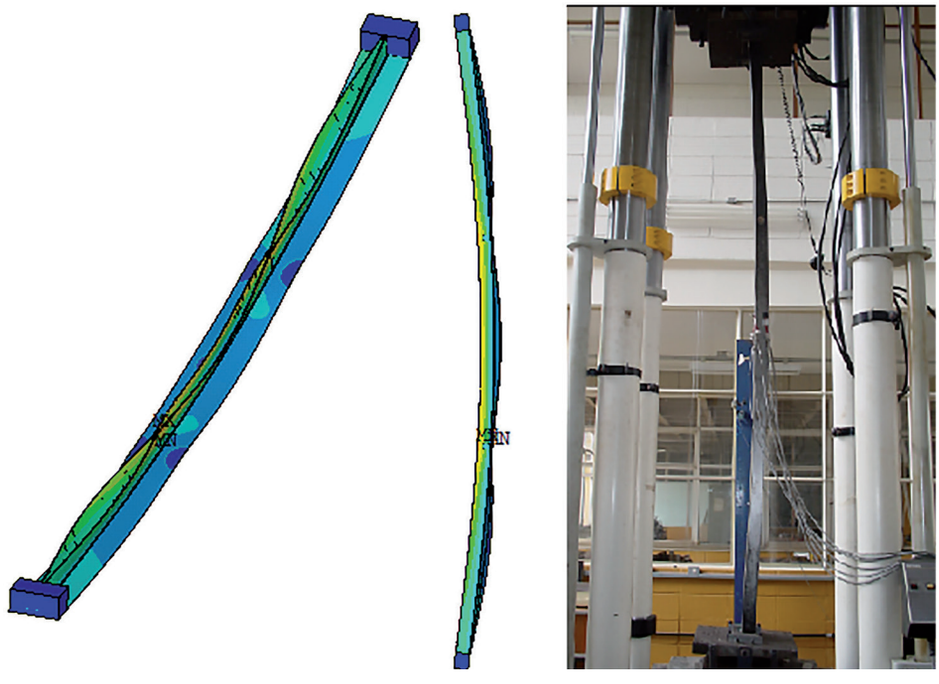

Figure 6
Deformed shape to Lr = 2765mm: numerical model and experimental test from Chodraui *et al.* (2006).

4. Results

Aiming to consider the variability of the geometric imperfections, numerical models were analyzed with different imperfections magnitudes, whose final mean results are presented in Table 1. The main objective is to compare the results from numerical analyses with those obtained by using standard codes, in particular concerning the standard ABNT NBR 14762:2010.

Defining the collapse modes of these profiles is not simple, since they present a large interaction between their buckling modes. Furthermore, they are bars composed of two profiles and their structural behavior can be understood as intermediate between a T-section profile and two simple angles. Therefore, the following definitions are used here in order to simplify the identification of the buckling modes: (F) flexural buckling of the double angle – characterized by the cross-section translation and by the bending around the weak axis, similar to a T-section profile; (T) torsional buckling of the double angle – characterized by the cross-section rotation, similar to a T-section profile; (FT) flexural-torsional buckling of the double angle – characterized by both translation and rotation of the cross-section, similar to a T-section profile; and (L) local buckling of the double angle – characterized by the plate buckling of the flaps, which can be seen as the flexural-torsional buckling of the angles between packing plates.

4.1 Angles with a thickness equal to 3.0mm

Results obtained by numerical analysis of the members with a 60x60x3.0 mm cross section are presented in Table 1a. Also, in Figure 7, there can be seen the deformed configuration of some modeled members

containing two packing plates at the time of their collapse.

Table 1
Results of the numerical analysis

Packing plates	Profile 60x60x3.0 – **Table 1a**				Profile 60x60x1.5 – **Table 1b**			
	L_r (mm)	$N_{FEM,m}$ (kN)	Buckling Mode	$N_{n,NBR}$/ $N_{FEM,m}$	L_r (mm)	$N_{FEM,m}$ (kN)	Buckling Mode	$N_{n,NBR}$ / $N_{FEM,m}$
0	380 (λ_x=20)	116.4	L	0.83	575 (λ_x=30)	41.2	L	0.30
1		133.0	F* + T + L	0.73		48.0	F* + L	0.26
2		141.8	F* + T + L	0.68		49.4	T + L	0.25
0	755 (λ_x=40)	105.6	L	0.91	1055 (λ_x=55)	34.6	L	0.36
1		113.1	F + T* + L	0.85		40.1	F + T* + L	0.31
2		123.4	F + T + L	0.78		39.5	F + T* + L	0.31
3		-	-	-		39.4	F + L	0.31
0	1325 (λ_x=70)	80.5	L	1.17	1625 (λ_x=85)	24.2	L	0.51
1		98.3	F + T* + L	0.96		31.1	F + FT* + L	0.40
2		102.7	F + T* + L	0.92		31.7	F + FT* + L	0.39
3		111.7	F + T + L	0.84		38.2	F + FT + L	0.32
4		-	-	-		38.1	F + FT + L	0.32
0	1890 (λ_x=100)	59.2	L	1.53	2200 (λ_x=115)	17.1	L	0.71
1		89.2	F + L	1.01		24.1	F + FT + L	0.51
2		93.5	F + FT* + L	0.97		24.6	F + FT + L	0.50
3		101.6	F + FT + L	0.89		29.3	F + FT + L	0.42
4		105.5	F + FT + L	0.86		31.0	F + FT + L	0.39
0	2460 (λ_x=130)	44.7	L	1.85	2775 (λ_x=145)	12.6	L	0.95
1		78.0	F + FT* + L	1.06		19.4	F + FT + L	0.62
2		82.2	F + FT* + L	1.01		20.3	F + FT + L	0.59
3		93.2	F + L	0.88		24.1	F + FT + L	0.50
4		97.4	F + L	0.85		24.2	F + FT + L	0.50
0	3030 (λ_x=160)	34.7	L	2.03	-	-	-	-
1		67.1	F + L	1.05		-	-	-
2		67.8	F + FT + L	1.04		-	-	-
3		79.8	F + FT + L	0.88		-	-	-
4		84.4	F + FT + L*	0.83		-	-	-

L_r – length of member (Figure 1); λ_x – slenderness ratio; * Buckling mode little pronounced.

$N_{n,NBR}$ – axial compression strength referred to design via standard ABNT NBR 14762;

$N_{FEM,m}$ – mean value of axial compression strength obtained from numerical analysis.

Unlike the models analyzed under axial compression, the flexural-torsional buckling is not predominant in these profiles (t = 3.0mm) when they are under eccentric compression. Except for low slenderness members, where the torsional modes were more clearly observed, the flexural buckling around the lower inertia axis (weak axis) is, together with local instabilities, the main fact responsible for the collapse. However, when increasing the amount of packing plates, noted is that the flexural-torsional buckling mode becomes more important to the stability of the member, although it is not as clear as the member bending, as shown in Figure 8b. Thus, it is evident that the load eccentricity is influential on the deformation trajectories and consequently on the profile strength.

In cases of members without packing plates, the behavior is equivalent to the two simple angles working individually, without any interaction with each other, resulting in a characteristic flexural-torsional buckling of the single angles under compression (Figure 8a). Such behavior implies interference on member resistance, whose values of axial compression strength are considerably below those results presented for the member containing one or more packing plates.

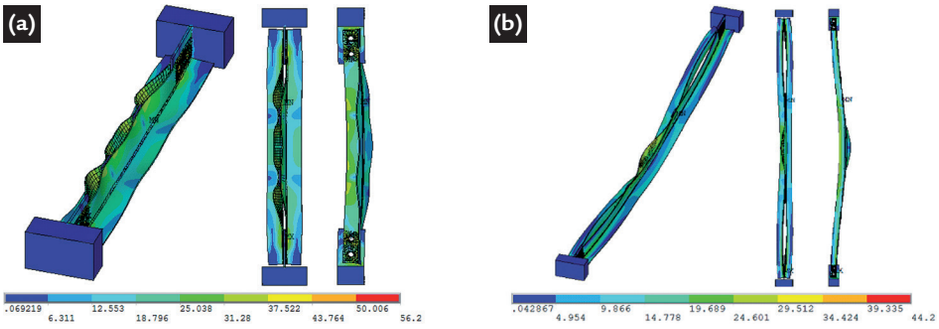

Figure 7
von Mises stresses (kN/cm^2) and deformed shape (enlarged scale) in the resistance limit of the member (a) L_r=755mm and (b) L_r=2460mm – *Section 60x60x3.0* (*two packing plates*).

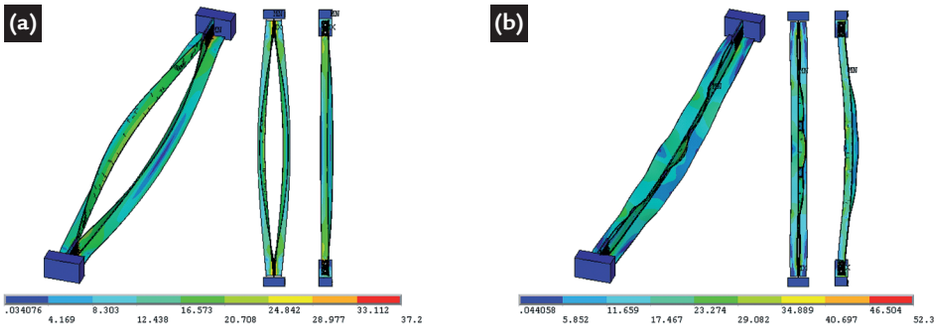

Figure 8
von Mises stresses (kN/cm^2) and deformed shape (enlarged scale): (a) member without packing plates and (b) member with four packing plates – *Section 60x60x3.0*.

In Figure 9, the mean values of strength ($N_{FEM,m}$) obtained by using numerical models are shown. The figure also shows curves relative to the stipulations of standards ABNT NBR 14762:2010 and ANSI/AISI S100 (2012) about the nominal compression strength of the members analyzed as a function of their length. Considering the fact that the bolted connection does not work as a perfectly clamped link, or even as a pinned support, the members were considered under two different conditions of linking: pinned ends bar (K_x=K_y=1.0); and semi-rigid ends bar relative to the axis of lowest inertia (K_x=0.8 e K_y=1.0) – Figures 10a and 10b, respectively.

Additionally, in the same Figure 9 are also presented the curves referring to the design of those members applying standard ABNT NBR 14762:2010 and ANSI/AISI S100 (2012), and designed as **NBR-FT** and **AISI-FT**, respectively, considering flexural buckling and flexural-torsional buckling. Also, **NBR** and **AISI-F** curves relative to the design of the members applying ABNT NBR 14762:2010 and ANSI/AISI S100 (2012) are presented, considering just buckling by bending of lower axis (hypothetic situation). The terms P0, P1, P2, P3 and P4 are relative to the numerical results of the members that have from zero to four packing plates, respectively. Notice that the curves resulting from the procedures of standard codes (NBR-FT and AISI-FT) have more adequate approximation when compared with numerical results, if connections are considered as semi-rigid (K_x=0.8), except for the cases without packing plates, as will be discussed later. Another important aspect observed is that the values of axial compression strength forecasted by code prescriptions for members with lower global slenderness resulted as being quite conservatives.

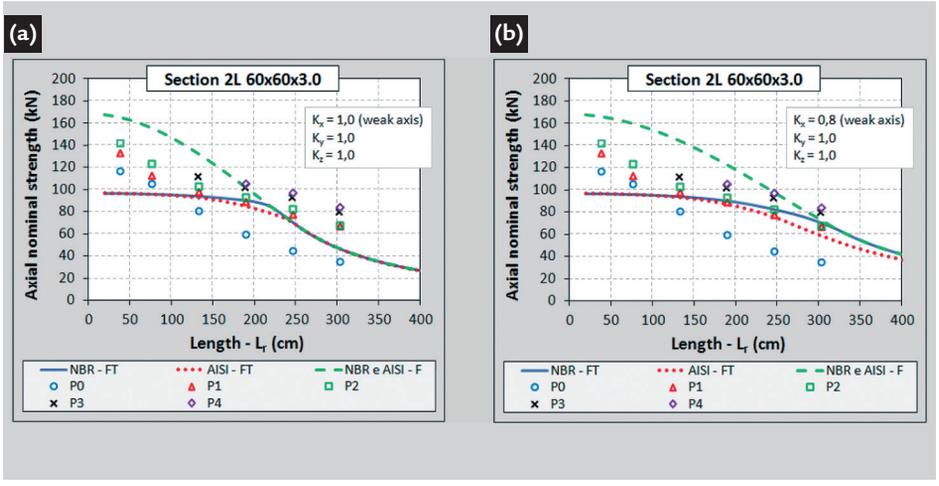

Figure 9
Numerical results and code predictions: (a) pinned end bar and (b) semi-rigid end bar.

4.2 Angles with a thickness equal to 1.5mm

Results obtained by numerical analysis of the members with a 60x60x1.5 mm cross section are presented in Table 1b. With respect to profiles considering a 1.5 mm thickness angle, the numerical results show an important interaction between three typical instability modes on monosymmetric members, i.e, flexural, flexural-torsional and local buckling. Considering those profiles, the predominance of one mode relative to another changes as function of the bar length, as can see in the examples in Figure 10 (results of members containing two packing plates).

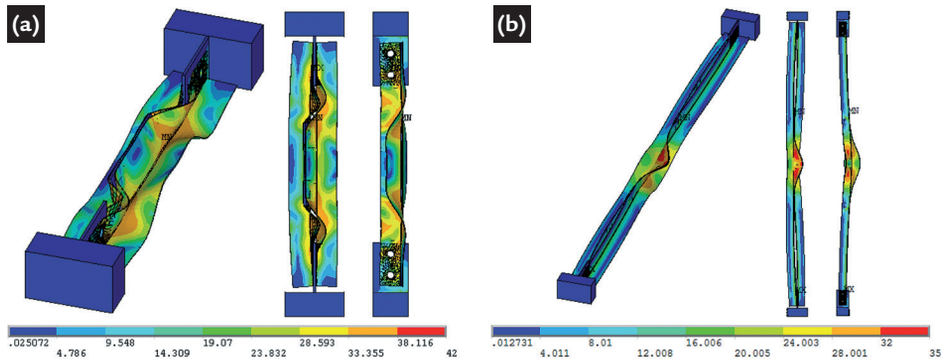

Figure 10
von Mises stresses (kN/cm²) and deformed shape (enlarged scale) in the resistance limit of the member (a) L_r=575mm and (b) L_r=2200mm – *Section 60x60x1.5 (two packing plates).*

Similar to the previous case (t = 3.0mm), the eccentric loading favors occurrence of flexural modes for the profiles. However, the decrease of the torsional moment of inertia, resultant from the thinness of the plates (t = 1.5mm), led to greater influence of the flexural-torsional buckling. Furthermore, the increase of the local slenderness makes them more susceptible to localized instabilities (flexural-torsional buckling of the insulated angles between packing plates), especially close to the center of the bar, where the most intensive bending moments occur due to the geometric imperfections and to the load eccentricity. As in the previous case, increasing the number of packing plates leads to the reduction of isolated behavior of the angle components of the member, which tends to work like an unique bar (behavior is close to a T-section member), similar to presented in Figure 8.

In Figure 11, the strength values (N_{FEM}) obtained by numerical models are presented, as well as the predictions of both standard codes ABNT NBR 14762:2010 and ANSI/AISI S100 (2012). For the graphics caption, the same definitions presented before are valid. When decreasing the plate thickness, it is observed that the results of axial compression strength, evaluated according to curves NBR-FT and AISI-FT, are significantly lower when compared to results of the numerical analysis, which tend to intermediate values for the flexural and flexural-torsional curves. In this case, it is possible to note that the effective length factor K_x = 0.8 does not reduce the difference found between the theoretical and numerical results, because the analyzed profile considers the slenderness range of values whose design is subdued by flexo-torsion instead of the flexion.

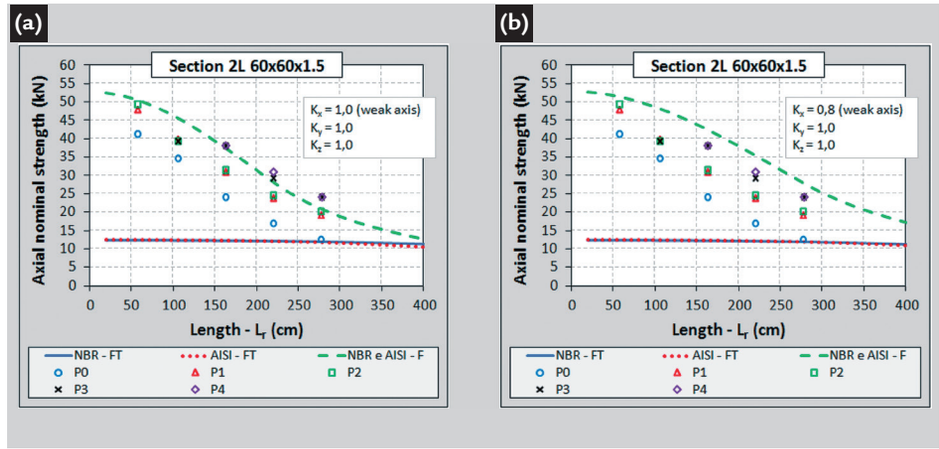

Figure 11
Numerical results and code predictions: (a) pinned end bar and (b) semi-rigid end bar.

Despite both the numerical and experimental results show the flexural-torsional buckling as one of the main causes responsible for the failure of most of the analyzed profiles, notice that axial strength values tend to follow the curves relative to flexural buckling (NBR e AISI-F) in cases with high local buckling slenderness. Thus, such results showed significant deviations relative to the designed curves resulting from standard codes (NBR-FT curves and AI-SI-FT).

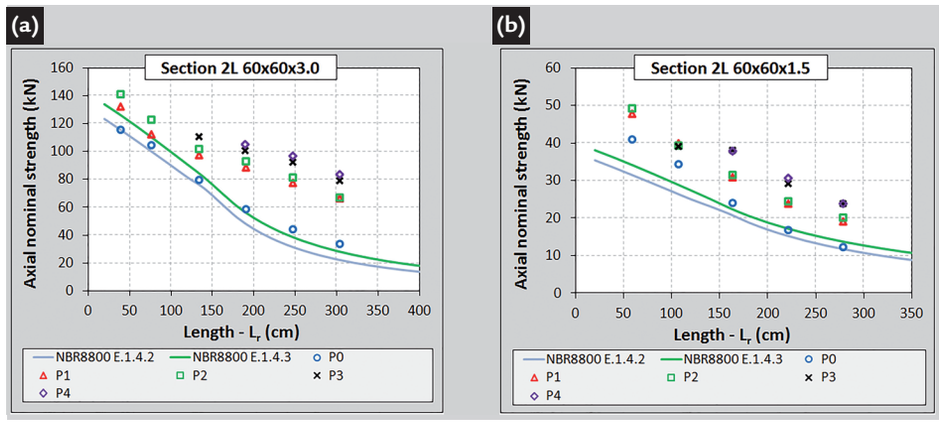

Figure 12
Numerical results and predictions of NBR 8800:2008 for two angles linked by one flap.

Finally, for the case of the members analyzed without packing plates, the results were compared to the standard code predictions (ABNT NBR 8800:2008) for simple angles connected by one of the flaps. This comparison can be seen in the Figure 12, where one can notice good agreement between those curves with numerical results for the case without packing plates (points designed as "P0"), signalizing the possibility of applying this methodology for cold formed angle design.

It is noted that the increasing of the number of packing plates results in a substantial increasing of the strength, especially when changing the number of packing plates from even to odd, as shown in the Tables 1a and 1b, as well as in Figure 12. In other words, the numerical results indicate that such members have their compression strength substantially increased when there is inserted one packing plate at half of its length.

5. Conclusions

The results indicate that the values of compression strength forces, obtained according to standard codes ABNT NBR 14762:2010 and ANSI/AISI S100 (2012), may be very conservative for the double angles back-to-back, mainly in the cases of lower global slenderness. The differences between the code predictions and the results obtained are much bigger when increasing the local buckling slenderness (width/thickness ratio) of the angle component of the member. Furthermore, whereas the numerical results indicate the flexural-torsional buckling as one of the main reasons responsible for the collapse of several analyzed members, it is noted that the results for compression strength force tend to have intermediate values for the curves relative to the flexural buckling and flexural-torsional buckling, following the trend of the flexural buckling curve in some cases. Therefore, the present work suggests more research about this type of profile, including other compositions of the angles (cross and batten sections), with the objective of establishing new code procedures promoting safety, as well as an economic design for the members composed by a double angle.

Additionally, the number and the distribution of packing plates are very important in the compression strength forces and in prevailing instability modes of the members. In this context, the use of one packing plate in the middle of the bar length shows to be the choice for a more indicated configuration relative to increasing the bar compression strength. For the cases of members without packing plates, numerical analysis indicates that the design proposed by ABNT NBR 8800:2008 for the case involving angles under compression connected by one flap can also be applied to cold formed angles.

References

ABNT NBR 8800 (2008). Brazilian Association of Standards and Techniques: Design of steel and composite structures for buildings. Rio de Janeiro: ABNT.

ABNT NBR 14762 (2010). Brazilian Association of Standards and Techniques: Design of cold-formed steel structures. Rio de Janeiro: ABNT.

ANSI/AISI S100 (2012). American Iron and Steel Institute. North American specification for the design of cold-formed steel structural members. Washington: AISI.

CHODRAUI, G. M. B. ***Theoretical and experimental analysis of cold-formed steel members under compression***. São Paulo, Brazil: School of Engineering at São Carlos, University of Sao Paulo, 2006. (Ph.D. Thesis).

CHODRAUI, G. M. B., SHIFFERAW, Y., MALITE, M., SCHAFER, B. W. ***Cold-formed steel angles under axial compression. Recent research and developments in cold-formed steel design and construction.*** In: INTERNATIONAL SPECIALTY CONFERENCE ON COLD-FORMED STEEL STRUCTURES, 18. Orlando, USA, Oct. 2006. Rolla, Missouri, USA: Missouri University of Science & Technology, 2006.

HANCOCK, G. J., YANG, D. ***Numerical simulation of high strength steel lipped-channel Columns***. Sydney, Australia: Department of Civil Engineering, University of Sydney, 2004.

LEAL, D. F. ***About cold-formed double angles back-to-back under compression***. São Carlos: School of Engineering at São Carlos, University of Sao Paulo, Brazil, 2011. (Thesis).

SCHAFER, B. W., PEKÖZ, T. Computational modeling of cold-formed steel: characterizing geometric imperfections and residual stresses. ***Journal of Constructional Steel Research,*** v.47, p. 193-210, 1998.

SWANSON ANALYSIS SYSTEMS INC. (SAS). ANSYS Reference Manual. v.13.

Received: 06 March 2017 - Accepted: 09 May 2017.